Intensity Ratios of *H* Lines: Departures from the Ideal Conditions in the Range of Laser-Induced Breakdown Spectroscopy Experiments

A. CRUZADO* and H. O. DI ROCCO

Facultad de Ciencias Astronómicas y Geofísicas, Universidad Nacional de La Plata, Paseo del Bosque s/n, 1900, La Plata, Argentina (A.C.); and Instituto de Física Arroyo Seco (IFAS), Universidad Nacional del Centro, Pinto 399 - B7000GHG - Tandil and CONICET, Argentina (H.O.D.R.)

In the present paper we analyze the behavior of H line intensity ratios with electron density and electron temperature in intermediate-density plasmas. We analyze the influence on the line intensity ratios of (1) the departures from local thermodynamic equilibrium (LTE) of the level population ratios, (2) the plasma opacity, and (3) the lowering of the ionization potential. We look, particularly, at the lines H_α, H_β, H_γ, and H_δ and the energy levels involved in the corresponding atomic transitions for their use as diagnostics in laser-induced breakdown spectroscopy (LIBS) experiments. One important conclusion is that, for typical values of the plasma dimension and the electron temperature taking place in LIBS, i.e., $L = 1$ mm and $T_e = 10\,000$ K, respectively, the intensity ratios H_β/H_α, H_γ/H_α, and H_δ/H_α depart from the ideal values by less than 10% in the interval 0.65×10^{14} part/cm^3 $\leq N_{HI} \leq 3.6 \times 10^{17}$ part/cm^3, which means 1×10^{14} part/cm^3 $\leq N_e \leq 1 \times 10^{16}$ part/cm^3 for a gas of pure hydrogen. For higher densities, the departures from ideal conditions increase very quickly due to opacity effects.

Index Headings: **Laser-induced breakdown spectroscopy; LIBS; Hydrogen; Plasma spectroscopy; Plasma diagnostics.**

INTRODUCTION

Hydrogen lines in the visible range are useful for plasma diagnostics, particularly for laser-induced breakdown spectroscopy (LIBS) experiments. Their intensity ratios provide information about the electron temperature T_e, the line widths are proportional to the electron density N_e, and the entire profile gives information about the plasma processes. In general, studying the spectroscopic properties of a plasma (both astrophysics and laboratory plasmas), involves at least the following questions: (1) the population distributions (departures from local thermodynamic equilibrium (LTE) conditions), (2) the radiation transport and the opacity effect (plasma thickness), (3) the lowering of the ionization potential, (4) the plasma homogeneity (or inhomogeneity), and (5) the variations in time. In the present work, the main problem to be addressed can be stated in the following terms: given the electron temperature and density, how much does the quotient between the intensities of two lines depart from the simple formula given for both LTE *and* a thin source? In the particular ideal case, the intensity ratio for two emission lines $p \rightarrow o$ and $v \rightarrow u$ is given by

$$R_{\text{ideal}}^{\text{I}} = \frac{I_{po}}{I_{vu}} = \frac{I_{po}^{\text{peak}}\Gamma_{po}}{I_{vu}^{\text{peak}}\Gamma_{vu}} = \frac{g_p f_{po}\omega_{po}^3}{g_v f_{vu}\omega_{vu}^3}\exp(\beta_{vp})\frac{\Gamma_{po}}{\Gamma_{vu}} \qquad (1)$$

where g is the level of multiplicity, f is the emission oscillator strength, ω is the emission frequency, Γ is the line width, and the exponent β_{vp} is defined as: $\beta_{vp} = (E_v - E_p)/kT$. A general answer for homogeneous plasmas was given in Refs. 1 and 2, and the following expression was found for the peak intensity ratio:

$$R_{\text{I}} = \frac{I_{po}^{\text{peak}}}{I_{vu}^{\text{peak}}} = \frac{\omega_{po}^3}{\omega_{vu}^3}P(C_{\text{T}}, x)G(\alpha, \beta) \qquad (2)$$

where $P(C_{\text{T}}, x)$ is a function of the absorption coefficients κ_{op} and κ_{uv}, and $G(\alpha, \beta)$ is a function of the level populations. The explicit expressions for $P(C_{\text{T}}, x)$ and $G(\alpha, \beta)$ functions can be found in the above cited references[1,2] and a very brief summary is given below in the following section.

A quasi-stationary approach for hydrogen is given in the pioneering works of Bates et al.[3,4] New experimental and numerical works about hydrogen lines were recently published.[5,6]

Since the solution of this problem in all generality presents physical and mathematical difficulties, it is necessary to make some simplifications in order to obtain simple criteria that could be of practical interest to those working in LIBS diagnostics. The assumptions used in our work to simplify it refer to:

(1) Homogeneity of the source. Whereas this condition looks somewhat restrictive, we take into account that when LIBS techniques are used for the study of traces and pollutants, they look at the plasma regions where the spectral lines show no dips. The quantification using lines with dips is practically impossible. Actually, the plasma is viewed with an adequate optical system, spatially filtered, and the information is not collected from the entire volume.[7]

(2) Steady state. Concerning this point, we must point out that we refer to plasmas observed with a box-car system, 1–1.5 μs after the plasma ignition and in a temporal gate of 30–50 ns. In this short interval time all the parameters characterizing the plasma are almost constant.

(3) Atomic processes. We have considered electron–ion and photon–ion interactions. We have neglected heavy particle interactions because we are interested in intermediate-density plasmas, for which the rates of this kind of process are much lower than electron–ion ones. Also, we could prove that, at the lower electron densities considered in this work, for which the heavy particle interactions would have some importance, the numerical results depend on the particular expressions used to calculate the electron collisions. Therefore, because of the uncertainty about the results at the lower densities and because we are interested mainly in their general trends with physical parameters rather than exact values, we prefer, in this instance, not to introduce more complexity to the problem.

Received 7 March 2007; accepted 28 June 2007.

* Author to whom correspondence should be sent. E-mail: acruzado@fcaglp.fcaglp.unlp.edu.ar.

0003-7028/07/6110-000000$2.00/0

(4) Plasma composition. It is frequent to consider an astrophysical plasma made of pure hydrogen and it is justified depending on the particular spectral feature in which we are interested. In this case, the number of free electrons and the number of neutral H atoms absorbing a given frequency are closely bound, depending on the temperature of the medium. In LIBS experiments, we do not deal with a plasma of pure hydrogen. In real experiments the H is a trace, and the free electrons come, also, from elements, other than hydrogen. In this case, the electron density does not necessarily reflect the H atom concentration. We have built a theoretical model for a gas of pure hydrogen and we have illustrated the behavior of level population and intensity line ratios as functions of electron density, which is the usual physical variable, in the paper. In the last section we show what it means in terms of H atom concentration and medium opacity.

With respect to the election of a hydrogen plasma for discussing LIBS problems, we can cite the work of Colona et al.,[8] in which it is stated that once the gaseous plasma is formed, its general behavior does not strongly depend on the chosen system.

Therefore, we deal with a homogeneous gas of pure hydrogen by adopting for the atomic model a number of bound levels permitted by the lowering of the ionization potential and a continuum. We consider a collisional radiative steady-state (CRSS) model[9] and we set the statistical equilibrium equations taking into account all the electron–ion and photon–ion processes that actually contribute to the population and depopulation of the atomic energy levels. We obtain the general behavior and trends of the level population and line intensity ratios with varying parameters such as electron temperature (T_e) and electron density (N_e), which are the standard parameters by which to characterize a laboratory plasma under general (non-LTE) conditions. We analyze, separately, the effects on the level population and line intensity ratios of the medium opacity and the lowering of the ionization potential.

In particular, we pay attention to the lines H_α, H_β, H_γ, and H_δ, which are useful for plasma diagnostics, and to the populations of the H energy levels with $n = 2$–6 from which they arise.

Thus, posing the problem in a very general context, our results permit the establishment of the physical conditions under which an ideal (equilibrium and thinness) state could be assumed within a given percent, compatible with experimental uncertainties as involved in the measurements of line intensity ratios.

Because we are interested mainly in LIBS applications, we work with temperature and density values within generally accepted limits for these experiments. Consequently, we make the plasma parameters vary in the intervals $1 \times 10^4\ \mathrm{K} \leq T_e \leq 2 \times 10^4$ K, and $1 \times 10^{14}\ \mathrm{part/cm^3} < N_e < 1 \times 10^{19}\ \mathrm{part/cm^3}$.

A BRIEF SUMMARY OF THEORETICAL EXPRESSIONS

In our model (see Refs. 1 and 2) the departure of the population ratios from LTE values is described by a parameter α_{nl}. Because other authors (particularly in astrophysics) use, for the same purposes, a parameter called b_{nl}, which is the inverse of our α_{nl}, in this paper we adhere to this latter custom. For a two level system n and l, assuming $E_n > E_l$:

$$\frac{N_n}{N_l} = b_{nl}\left(\frac{N_n}{N_l}\right)^* = b_{nl}\left(\frac{g_n}{g_l}\right)e^{-\beta_{nl}}$$

where the factor b_{nl} summarizes the deviation from thermodynamic limit due, in principle, to radiative processes, inclusively in a transparent medium. For a multilevel system the general expression can be found in Ref. 2, although, through numerical calculations, b_{nl} can be found directly from $b_{nl} = (N_n/N_l)/(N_n/N_l)$. The superscript "*" identifies quantities in LTE. Furthermore, opacity and lowering effects modify the physical significance of b_{nl} as just the influence of the radiative processes.

To study the influence of optical thickness on the line intensity ratios, we consider four arbitrary levels, $|p\rangle$, $|o\rangle$, $|v\rangle$, and $|u\rangle$, and two lines, $p \rightarrow o$ and $v \rightarrow u$, with intensities denoted by I_{po} and I_{vu}, respectively. We always assume that $E_p > E_o$ and $E_v > E_u$, but there are no restrictions between the states p and v nor between o and u. For a fixed plasma length, L, the integrated intensity is given in SI units by the area under the curve:[10]

$$I_{po}(\omega) = \frac{h}{8\pi^4 c^2}\frac{\omega_{po}^3\{1 - \exp[-\kappa_{op}(\omega)L]\}}{\left(\frac{g_p N_o}{g_o N_p} - 1\right)} \tag{3}$$

where N_o, N_p, g_o, and g_p are the populations and the statistical weights of the o and p levels, respectively, ω_{po} is the frequency of the line, and κ_{op} is the absorption coefficient, defined by:

$$\kappa_{op}(\omega) = \frac{\pi e^2}{2\varepsilon_o mc} f_{op} N_o\left(1 - \frac{g_o N_p}{g_p N_o}\right)\wp(\omega) \tag{4}$$

where $\wp(\omega)$ is the line shape and f_{op} is the *absorption* oscillator strength; in the peak of the profile $\wp(\omega) \sim 1/\Gamma$. Writing similar equations for $I_{vu}(\omega)$ and κ_{uv}, and calling $x \equiv \kappa_{op}L$, $y \equiv \kappa_{uv}L$, and defining $C_T \equiv y/x = \kappa_{uv}/\kappa_{op}$, the ratio of peak intensities results in:

$$R_I = \frac{I_{po}^{\mathrm{peak}}}{I_{vu}^{\mathrm{peak}}} = \left(\frac{\omega_{po}}{\omega_{vu}}\right)^3\left[\frac{1 - \exp(-x)}{1 - \exp(-C_T x)}\right]\left[\frac{\exp(\beta_{vu})/b_{vu} - 1}{\exp(\beta_{po})/b_{po} - 1}\right] \tag{5}$$

Introducing two auxiliary functions, $P(C_T, x)$ and $G(b, \beta)$ (the first and second square parenthesis), Eq. 5 can be rewritten as

$$R_{I,} = \left(\frac{I_{po}^{\mathrm{peak}}}{I_{vu}^{\mathrm{peak}}}\right)_{\mathrm{general}} = \left(\frac{\omega_{po}}{\omega_{vu}}\right)^3 P(C_T, x)G(b, \beta) \tag{6}$$

Clearly, the departure of the ideal case (in both LTE and thinness) can be quantified by the quotient

$$Q(po, vu) = \frac{(I_{po}^{\mathrm{peak}}/I_{vu}^{\mathrm{peak}})_{\mathrm{general}}}{(I_{po}^{\mathrm{peak}}/I_{vu}^{\mathrm{peak}})_{\mathrm{ideal}}} = \frac{P(C_T, x)G(b, \beta)}{(g_p f_{po}\Gamma_{vu}/g_v f_{vu}\Gamma_{po})\exp(\beta_{vp})} \tag{7}$$

Values of Q near unity indicate conditions close to the ideal ones, whereas departure from one or both of these ideal conditions are evidenced by Q values differing from unity.

THE ATOMIC MODEL

The Statistical Equilibrium Equations. Population distributions are studied using the collisional radiative steady state (CRSS) model.[9] This model is valid whenever the plasma characteristic time t_{pl} is larger than the time scale of atomic processes (t_a), i.e., $t_{pl} \gg t_a = 1/n_e\langle v\sigma\rangle$; this condition is valid for laser-generated plasmas in the nanosecond regime. The number of excited atoms in each atomic level can be determined by balancing the processes populating and depopulating each level. In a partially ionized plasma, the dominating mechanisms to be taken into account are spontaneous emission, induced radiative excitation and de-excitation, electron-impact excitation and de-excitation, radiative recombination, three-body recombination, and electron-impact ionization. Processes involving heavy particles are not considered here.

Thus, we can write for atoms excited to the nth level:

$$\sum_{m>n} N_m A_{mn} + \sum_{m\neq n} N_m B_{mn} J_{mn} + \sum_{m\neq n} N_m N_e C_{mn} + N^+ \left(\frac{n_n}{N^+}\right)^* R^R_{cn} + N^+ N_e^2 R^{3b}_{cn} = \sum_{m<n} N_n A_{nm} + \sum_{m\neq n} N_n B_{nm} J_{nm} + \sum_{m\neq n} N_n N_e C_{nm} + N_n N_e I^{Col}_{nc} \quad (8)$$

where the terms are defined as follows:

N_e:	electron number per volume unit in cm^{-3}
N^+:	ion number per volume unit in cm^{-3}
N_n and N_m:	number of excited atoms in the nth and mth level, respectively, in cm^{-3}
A_{mn}:	spontaneous emission probability for the $m \rightarrow n$ transition in s^{-1}
B_{nm} and B_{mn}:	induced radiative probability for the $n \rightarrow m$ and $m \rightarrow n$ transitions, respectively, in $cm^2\ erg^{-1}\ s^{-1}$
C_{nm} and C_{mn}:	rate coefficients in $cm^3\ s^{-1}$ for the electron-impact excitation and de-excitation as indicated by the sub-index
R^R_{cn}:	rate coefficients for radiative recombination in s^{-1}
R^{3b}_{cn}:	rate coefficients for three-body recombination in $cm^6\ s^{-1}$
I^{Col}_{nc}:	rate coefficients for the electron-impact ionization in $cm^3\ s^{-1}$
J_{mn}:	mean intensity of the radiation field for the $m \rightarrow n$ transition frequency in $erg\ cm^{-2}$

As before, the superscript "*" in $(N_n/N^+)^*$ denotes LTE values.

We have, in total, n_{max} equations like Eq. 8 for every bound level allowed by the lowering of the ionization potential, which is analyzed in the Lowering the Ionization Potential subsection below.

Furthermore, the following constraint equation, valid for steady-state systems, must be added to the above equations:

$$(N_1 I^{col}_{1c} + N_2 I^{col}_{2c} + \cdots)N_e = \left[(R^{3b}_{c1} + R^{3b}_{c2} + \cdots)N_e^2 + \left(\frac{N_1}{N^+}\right)^* R^R_{c1} + \left(\frac{N_2}{N^+}\right)^* R^R_{c2} + \cdots\right]N^+ \quad (9)$$

which states the equilibrium between ionizations and recombinations.

Rate Coefficients. The rate coefficients are taken from the literature as we explain below.

The spontaneous transition probability from an upper state m to a lower state n, A_{mn}, is calculated using the formalism of atomic theory.[11] The induced emission probability and the resonant photo-absorption coefficients, B_{nm} and B_{mn}, are connected to the Einstein A coefficient by means of well-known expressions.

For the calculation of the electron impact excitation rate coefficient we start from the general scaled expression:[12]

$$C_{nm} = K\left(\frac{\Delta E}{Ry}\right)^{1/2} \beta^{3/2} e^{-\beta} \int_0^\infty \frac{\sigma(u)}{\pi a_0^2}(u+1)d^{-\beta u}\mathrm{d}u \quad (10)$$

where $K = 2.18 \times 10^8\ cm^3\ s^{-1}$, $\beta = \Delta E/kT$, $u = (E - \Delta E)/\Delta E$, and a_0 is the Bohr radius. By proposing different expressions for $\sigma(u)$, we can attain different rates. We have tested different expressions from the literature, taking into account that for the experimental parameters found in LIBS experiments (relatively high N_e values and $T_e \sim 1$ eV) the results are not strongly dependent on such formulas. This is not the case for lesser densities, but this situation is not our concern in the present work. In short, we have used the expressions proposed by Vriens and Smeets.[13] The rate coefficients for the inverse process, the electron-impact de-excitation, are obtained by applying the detailed balance principle.

The number of spontaneous radiative recombinations to the n level is calculated by using the following expression:[14]

$$R^R_{cn} = 4\pi \int_{\nu_0}^\infty \frac{\alpha(\nu)}{h\nu}\frac{2h\nu^3}{c^2}\exp\left(-\frac{h\nu}{kT}\right)\mathrm{d}\nu \quad (11)$$

where $\alpha(\nu) = 2.81 \times 10^{29}\ g(\nu)Z^4/n^5\nu^3$ for hydrogenic ions.[14,15]

The electron-impact ionization rate coefficient is calculated by means of the Lotz's formula:[16]

$$I^{Col}_{nc} = 3 \times 10^{-6} T^{-3/2}\frac{1}{y}E_1(y) \quad (12)$$

where $y = I/kT$ and $E_1(y)$ is the exponential integral. This expression is still widely used because it is very simple and very good results have been obtained with it.[15] The relation between this process and the inverse process, three-body recombination, is defined by the detailed balance principle.

The radiation field, J, at the second term of the left and right sides of Eq. 8, is written as $J_\nu = B_\nu(T_e)(1 - e^{-\tau_\nu})$, where $B_\nu(T_e)$ is the Planck function evaluated at the line frequency ν and the electron temperature T_e, and τ_ν is the line opacity. In this paper τ_ν is taken as the optical thickness at the peak of a Lorentzian profile. Therefore, $\tau_\nu = \kappa_\nu N_m L/\Delta\nu$ can be written, where κ_ν is the absorption coefficient per atom at the m state, N_m is the lower state population, L is the path length, and $\Delta\nu$ is the

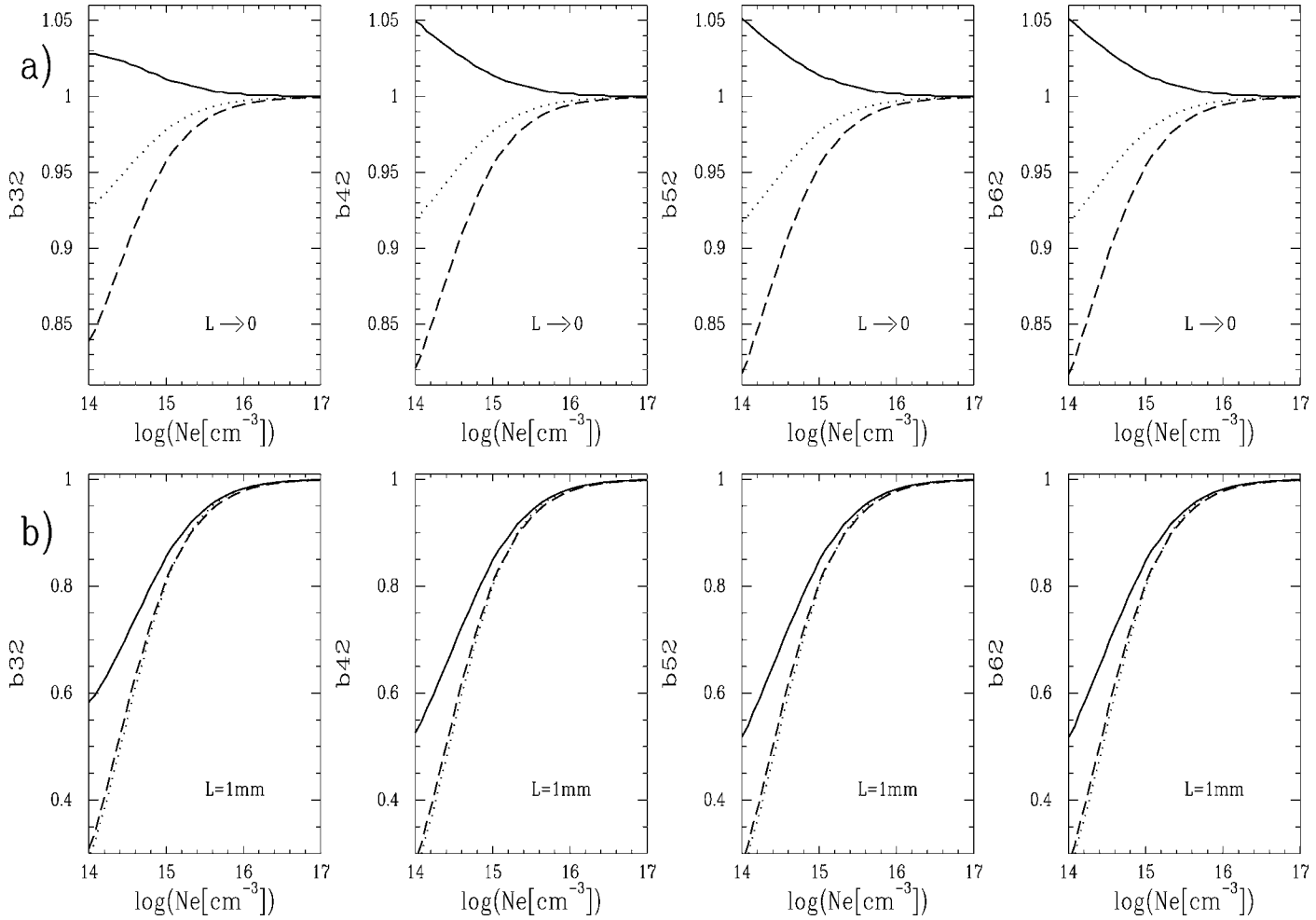

FIG. 1. (**a**) Coefficients b_{nl} for levels giving the lines H_α, ... , H_δ for a transparent media. b_{nl} is shown as a function of the decimal logarithm of N_e for different T_e values. Solid line: $T_e = 10\,000$ K, dotted line: $T_e = 15\,000$ K, dashed line: $T_e = 20\,000$ K. (**b**) The same as panel (a) for a medium with plasma dimensions $L = 1$ mm.

intrinsic half-width of the line profile. Because N_m is unknown at the beginning, we start the calculations by assuming a Boltzmann distribution. The N_m values obtained by solving the system of Eq. 8 together with Eq. 9 are introduced in a next iterative step until convergence is attained.

The Lowering of the Ionization Potential. Coulomb interactions give rise to the lowering of the ionization limit, ΔI, relative to the theoretical value for an isolated atom. Diverse criteria have been proposed over the years and several monographs deal with this subject.[15] They use two typical plasma lengths: the Debye radius $\rho_D[m] = (\varepsilon_0 kT/e^2 N_e)^{1/2} \approx 50\{T[K]/N[m^{-3}]\}^{1/2} m$ and the cell radius R_0 of the ion-sphere model, defined by the condition $(4\pi/3)R_0^3 N_i = 1$. Griem[15] suggests combining the different criteria into

$$\frac{\Delta I}{Ry} = z \min\left(\frac{2a_0}{\rho_D}, \frac{3a_0}{2R_0}\right) \qquad (13)$$

where Z is the charge of the resulting ion ($Z = 1$ in our case) and a_0 is the Bohr radius. Although it is obvious from their definitions that ρ_D depends on both N_e and T_e, R_0 depends only on the ion density.

Because it is not the purpose of this work to select one or the other criterion, only comparisons using the combined criterion given by Eq. 13 will be shown. Under the physical conditions in which we are interested, the lowering of the ionization limit of the H atom, ΔE_∞, varies in such form that we must use $\Delta E_\infty / Ry = 2a_0/\rho_D$.

Therefore, according to the previous paragraph, a maximal principal quantum number, n_{max}, for bound states must be considered, n_{max} being the largest n below the modified ionization limit.

The comparison between the population ratios with and without these corrections will be shown below.

RESULTS

In order to obtain the present results, a homogeneous layer of pure hydrogen consisting of neutral atoms, protons, and free electrons, and characterized by T_e and N_e, is considered in every case. In order to solve the system of Eq. 8 for N_n, $n = 1$, 2, ... , n_{max} together with Eq. 9, we build an $n_{max} \times n_{max}$ matrix where the level populations N_1, N_2, N_3 ... , are the unknown quantities. The matrix is solved by a standard elimination method.

Because the level populations are needed to evaluate the opacity, τ_ν, and then the exponential $e^{-\tau_\nu}$ in the expression of J, an iterative method is applied, as we have explained in the

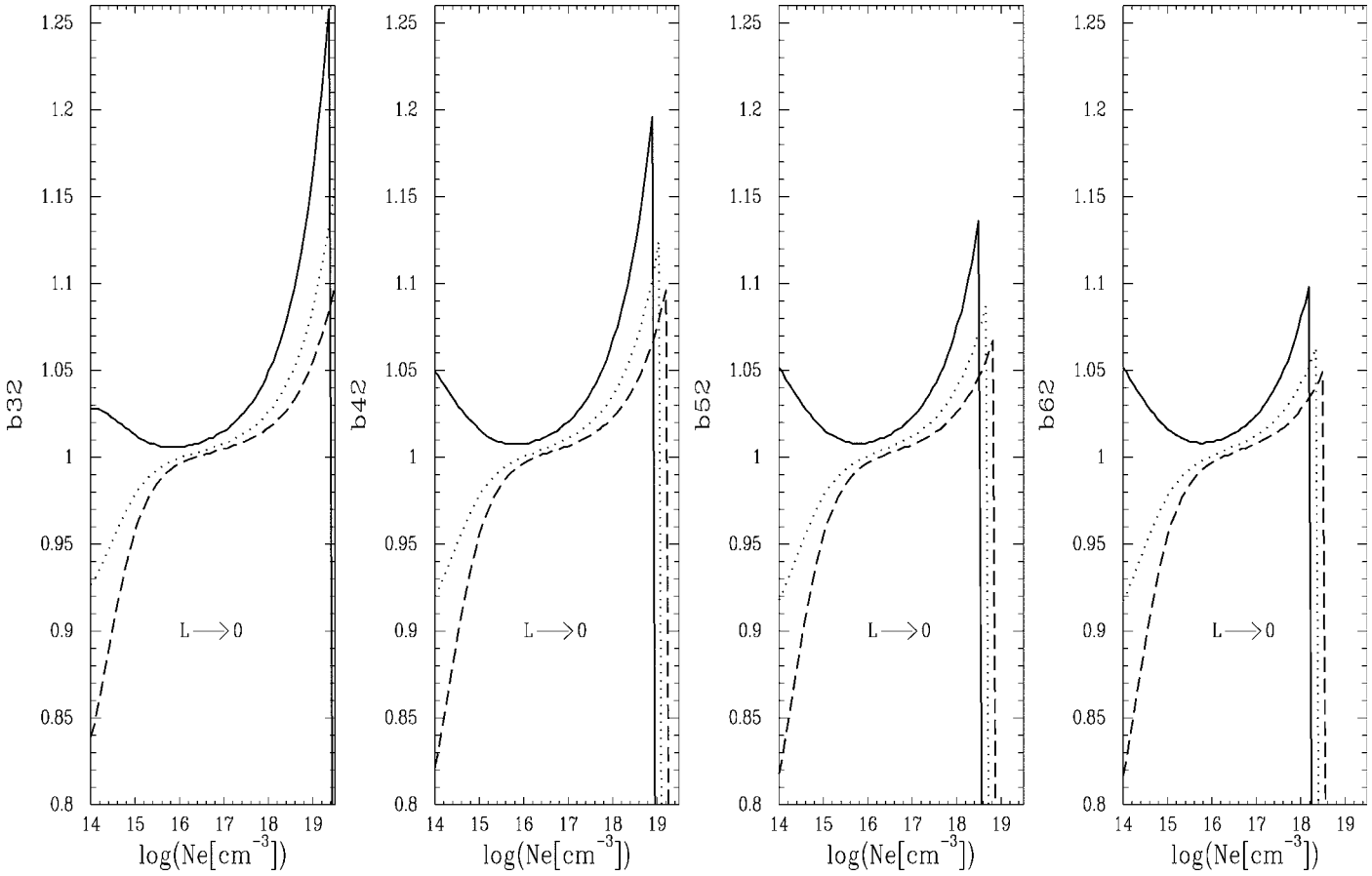

FIG. 2. The same as Fig. 1a, taking into account the lowering of the ionization potential.

former section, and the matrix is solved as many times as needed to reach convergence.

The energy level populations of the H atom are obtained for the range of values of the physical parameters in which we are interested, namely, $1 \times 10^4 K \leq T_e \leq 2 \times 10^4 K$, and 10^{14} part/cm^3 $< N_e < 1 \times 10^{19}$ part/cm^3. Then, the line intensity ratios are obtained by means of the theoretical expressions already summarized.

To see the influence on the population and intensity ratios of the medium opacity and of the lowering of the ionization potential, we consider, first, each of these effects separately. Obviously, this ideal case is not an achievable one; indeed, as the density increases, both opacity and lowering effects become noticeable together.

The main results reached from our calculations are shown in Figs. 1–6 and are analyzed in the following sections.

Population Ratios. In Fig. 1a the ratios $(N_3/N_2)/(N_3/N_2)^*$, ..., $(N_6/N_2)/(N_6/N_2)^*$ (that is, the coefficients b_{nl} defined above) are displayed as functions of N_e for different T_e values for a transparent medium. Figure 1a is not very interesting in itself, because, while the equilibrium is strictly achieved for high N_e values, departures from LTE for the lowest N_e values remain less than 15%, i.e., on the order of other experimental uncertainties. Also, we could prove that, at the lower N_e values, the numerical results depend on the particular expressions taken to represent the collisions, even though they show similar behavior with T_e and N_e. However, the population ratios are shown in order to see the effects of the opacity and the lowering of the ionization potential on them.

Opacity effects on population ratios are shown in Fig. 1b, where the same ratios as in Fig. 1a are displayed for an opaque medium with $L = 1$ mm. We see that the opacity effect on the population ratios is to reduce them with respect to the transparent case. For $N_e = 1 \times 10^{15}$ part/cm^3 and $T_e = 20\,000$ K, for example, N_3/N_2 departs from the equilibrium value by nearly 20% for a typical geometrical dimension used in LIBS experiments, whereas it departs less than 5% for a transparent medium. Photo-excitations from the ground level, which are absent in a transparent medium, overpopulate the $n = 2$ level and, consequently, the ratios N_n/N_2 are reduced. For $N_e > 1 \times 10^{16}$ part/cm^3, these effects are no longer observed. For this relatively high density value, the collisional processes determine the level populations.

The lowering effects on the population ratios are shown in Fig. 2. The ratios displayed in this figure are calculated assuming a transparent medium and taking into account the lowering of the ionization potential. A noticeable rise in the population ratios is observed for N_e values for which the equilibrium would be attained if no lowering was considered, with a fast decrease later on. A given bound level n, is, little by little, overpopulated as N_e increases and more and more higher bound levels become continuum energy levels. The higher the level n is, the more over-populated it is. Then, population ratios such as N_n/N_l with $n > l$ increase. This remains the case until

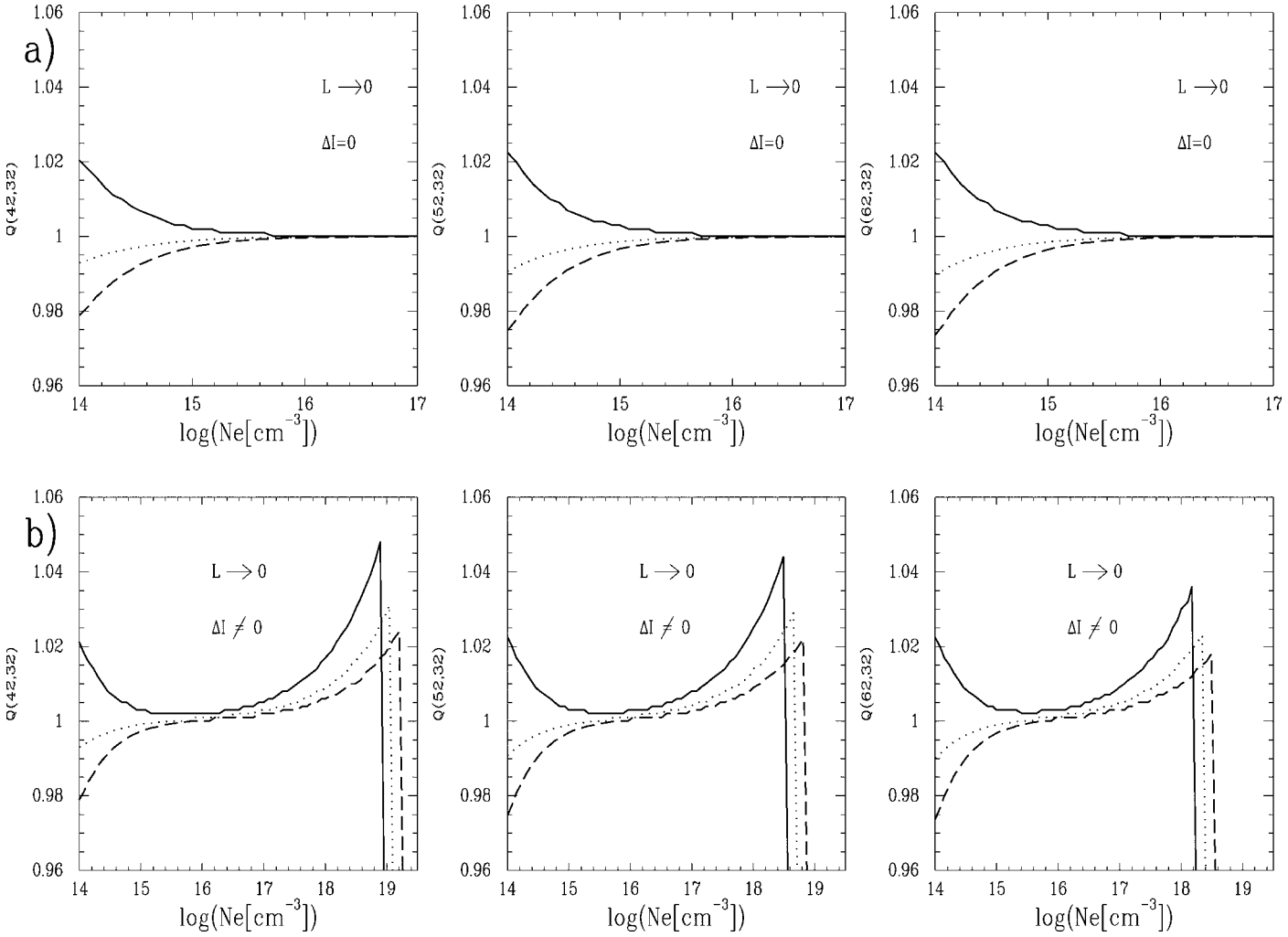

FIG. 3. (**a**) Q values for ratios $(H_\beta/H_\alpha)/(H_\beta/H_\alpha)^{id}$, $(H_\gamma/H_\alpha)/(H_\gamma/H_\alpha)^{id}$, and $(H_\delta/H_\alpha)/(H_\delta/H_\alpha)^{id}$ for a transparent media. Q is shown as a function of the decimal logarithm of N_e, for different T_e values, without taking into account the lowering of the ionization potential. Solid line: $T_e = 10\,000$ K, dotted line: $T_e = 15\,000$ K, dashed line: $T_e = 20\,000$ K. (**b**) The same as panel (a), taking into account the lowering of the ionization potential.

the level n, itself, does not exist any more as a bound level. Then, a fast decrease of the function b_{nl} occurs.

Line Intensity Ratios. The intensity of a spectral line depends, on one hand, on the intrinsic characteristics of the atomic transition (line frequency, oscillator strength, and statistical weights of the involved levels) and, on the other hand, on the physical conditions of the medium (N_e, T_e, and L), which determine the atomic level populations and the medium opacity. In this section we analyze the general behavior of the line intensity ratios with the physical conditions of the medium with respect to the same ratios under ideal conditions; ideal conditions, in this context, refers to LTE conditions and a transparent medium.

In Figs. 3a and 3b we draw the intensity ratios $(H_\beta/H_\alpha)/(H_\beta/H_\alpha)^{id}$, $(H_\gamma/H_\alpha)/(H_\gamma/H_\alpha)^{id}$, and $(H_\delta/H_\alpha)/(H_\delta/H_\alpha)^{id}$ (the Q values defined in the Theoretical Expressions section above) as functions of N_e for different T_e values, without and with lowering, respectively, for a transparent medium. As we expect from the theoretical expressions for two lines sharing the lower energy level, the line intensity ratio with respect to the ideal ratio equalizes the population ratio of the upper levels of the lines with respect to the LTE ratio. Therefore, $(H_\beta/H_\alpha)/(H_\beta/H_\alpha)^{id} = (N_4/N_3)/(N_4/N_3)^*$, $(H_\gamma/H_\alpha)/(H_\gamma/H_\alpha)^{id} = (N_5/N_3)/(N_5/N_3)^*$, and $(H_\delta/H_\alpha)/(H_\delta/H_\alpha)^{id} = (N_6/N_3)/(N_6/N_3)^*$ for a transparent medium.

In Figs. 4a and 4b we see the same ratios shown in Fig. 3 for an opaque medium with $L = 1$ mm. A logarithmic scale must be used in this case. The influence of the opacity on the line intensity ratios for $N_e > 1 \times 10^{16}$ part/cm^3 is impressive, both considering or not considering the lowering of the ionization potential. Actually, very small departures from ideal conditions, undetectable in the scale of Fig. 4 (less than 10%), also occur for $N_e < 1 \times 10^{15}$ part/cm^3. To understand this, let us analyze the Q dependence on the medium opacity. The Q factor depends on the opacity in two ways. On one hand, Q depends explicitly on the opacity in an exponential form ($P(C_T, x)$ function in Eq. 7). It originates the huge departures from the ideal case at high density values. On the other hand, Q depends implicitly on the opacity through the population ratios ($G(\alpha, \beta)$ function in Eq. 7). It originates small departures from the ideal case at low density values. We must take into account that at

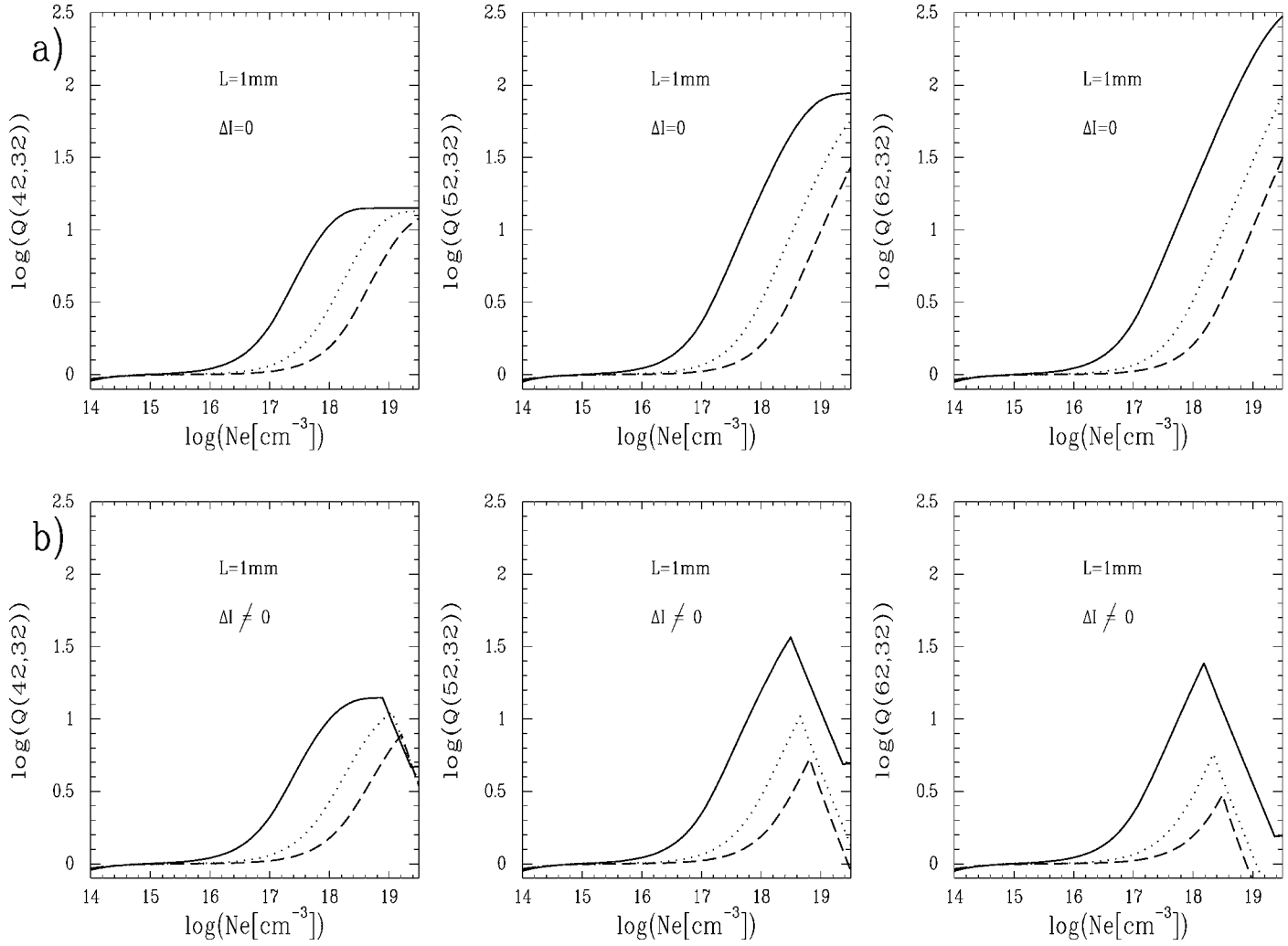

FIG. 4. (**a**, **b**) The same as Figs. 3a and 3b, respectively, for an opaque medium ($L = 1$ mm). Notice that, unlike Fig. 3, a logarithmic scale is used in both axes.

these low density values, population ratios depart from LTE values even for transparent media (see Figs. 1a and 1b).

In Fig. 5, returning to a linear scale, we see the above-cited ratios at a fixed $T = 10^4$ K for different plasma dimensions.

Regarding the lowering of the ionization potential, the Q dependence on it is only through the population ratios. Its effect on the ratios $(H_\beta/H_\alpha)/(H_\beta/H_\alpha)^{\rm id}$, $(H_\gamma/H_\alpha)/(H_\gamma/H_\alpha)^{\rm id}$, and $(H_\delta/H_\alpha)/(H_\delta/H_\alpha)^{\rm id}$, which is obviously observed at high density values, is to reduce them with respect to the values they would have if no lowering was considered. This fast decrease of $Q(op, vu)$ observed at high density values when the lowering of the ionization limit is taken into account (Figs. 3b, 4b, and 5) reflect the fact that the levels involved in the transitions, are, little by little, merging into the continuum as $N_{\rm e}$ increases and leave off being bound levels.

DISCUSSION AND CONCLUSION

The objective of our work is to establish the influence of all three effects, (1) the departures from LTE of the energy level populations, (2) the opacity of the medium, and (3) the lowering of the ionization potential, on the intensity ratios of H spectral lines and to compare them with the ratios obtained under LTE and thin source conditions for their use in the diagnostics of laser generated plasmas.

Even though the more direct experimental measurements are intensity ratios, the departures from LTE conditions of the energy level populations concern us in the measure that they affect the intensity lines. For that reason, the behavior of the b_{nl} coefficients and their departures from unity are displayed in Figs. 1 and 2 and are analyzed in the previous section. We conclude that the opacity of the medium and the lowering of the ionization potential affect the ratios $b_{nl} = N_n/N_l$ with $n > l$ in two different $N_{\rm e}$ ranges and in opposite directions: the opacity decreases the ratios, with respect to their values for a transparent medium, at the lower density values, while the lowering of the ionization potential increases the ratios, with respect to the ideal case without taking it into account, only at the higher density values.

Specifically regarding intensity ratios, our more important results are summarized in Figs. 3, 4, and 5, which are analyzed in the previous section, We infer that if the media can be considered nearly transparent (Fig. 3 and $L = 0.01$ mm in Fig. 5), Q values are nearly unity for all $N_{\rm e}$ values for which the energy levels involved in the transitions remain as bound levels, according to the corresponding lowering of the

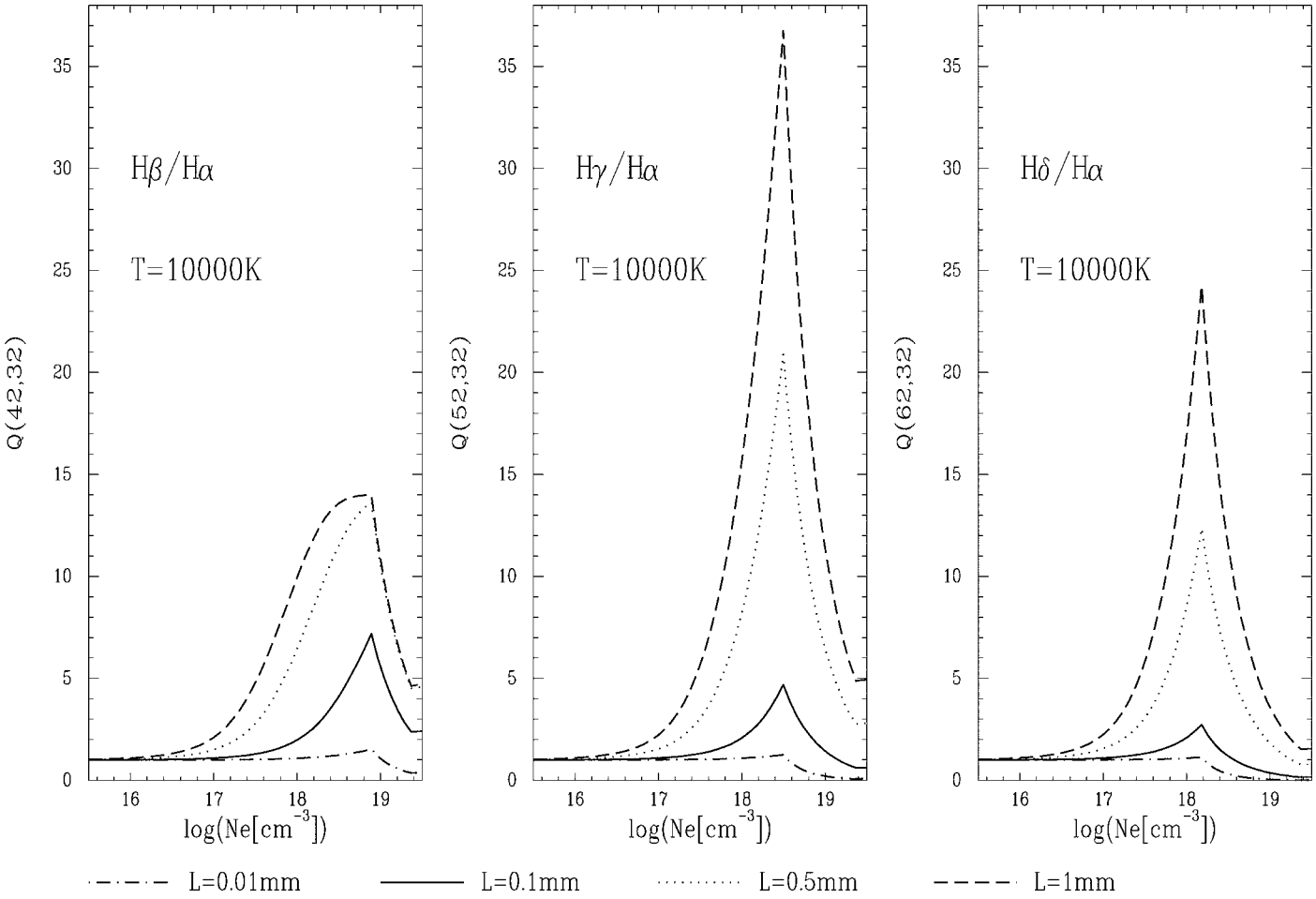

FIG. 5. Q values for ratios $(H_\beta/H_\alpha)/(H_\beta/H_\alpha)^{id}$, $(H_\gamma/H_\alpha)/(H_\gamma/H_\alpha)^{id}$, and $(H_\delta/H_\alpha)/(H_\delta/H_\alpha)^{id}$ at a fixed $T = 10\,000$ K using L as the variable parameter.

ionization potential. If $L \leq 0.01$ mm, for a typical T_e value of 10^4 K, Q is never departs from unity by more than 5% provided $N_e > 1 \times 10^{14}$ part/cm^3 (Fig. 3).

For an opaque medium, all Q values increase with respect to the ideal case, and huge departures from the ideal conditions are observed at high densities (Fig. 4 and Fig. 5). These deviations from ideal conditions observed at high density for an opaque medium by no means reflect deviations from LTE conditions, which are strictly met for high densities and high opacities. They are a direct consequence of the opacity.

It is worthwhile to clear up the definition of an opaque medium in terms of atom and electron numbers. The atomic level populations, on one hand, depend on both the total number of atoms and the number of free electrons, whether they are related or not. On the other hand, the optical thickness of the medium, with a very important physical meaning in the context of this paper, depends on the *density* of absorbing atoms and the plasma dimensions. In order to illustrate how the different parameters are related to each other and to the departures from ideal conditions, $Q(42, 32)$ is shown in Fig. 6 as a function of the electron density, N_e, the neutral atoms density, $N(HI)$, and the optical thickness at the frequency of the H_α line, $\tau(H_\alpha)$, for two different temperature values and two different path length values.

For typical values for the plasma dimension and the electron temperature for plasmas in air, $L = 1$ mm and $T_e = 10\,000$ K, respectively, the intensity ratios H_β/H_α, H_γ/H_α, and H_δ/H_α depart from the ideal values by less than 10% in the interval 0.65×10^{14} part/cm^3 $< N(HI) < 3.6 \times 10^{17}$ part/cm^3, which means 1×10^{14} part/cm^3 $< N_e < 1 \times 10^{16}$ part/cm^3 for a gas of pure hydrogen and $0.0045 < \tau(H_\alpha) < 0.23$ (Fig. 6a)). For higher densities, the departures from ideal conditions increase due to opacity effects, slowly at the beginning, and very fast afterwards. For higher values of T_e, as those reached when discharges are produced in partial vacuum, the intervals of atom number and electron number for which the intensity ratios depart from ideal values by less than 10% change (Fig. 6b)). Nevertheless, the condition $\tau(H_\alpha) < 0.23$ remains valid. In the same way, the intensity ratios depart by approximately 50% from the ideal values when $\tau(H_\alpha) = 1$, regardless of what the other parameters are. Huge departures from ideal conditions are observed for $\tau(H_\alpha) > 1$.

It is clear that this work can be generalized in several aspects, which we have mentioned in the Introduction as simplifications. Particularly, we are planning to improve our results by considering that in LIBS experiments the majority of the electrons come from the bulk material and the atmosphere, being N_e different from the proton density. Also, the temporal evolution due to the plasma expansion will be considered.

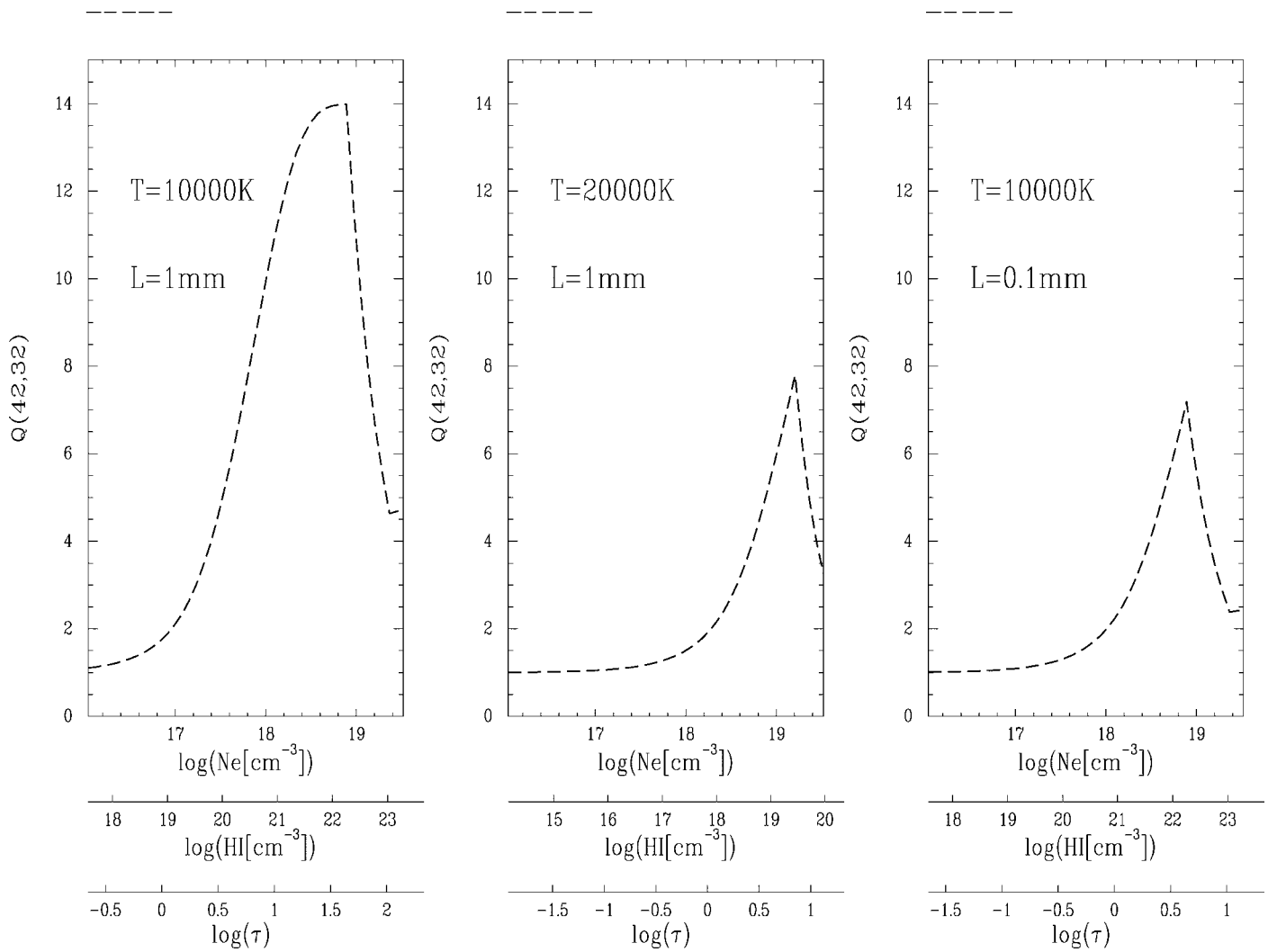

FIG. 6. Q values for the ratio $(H_\beta/H_\alpha)/(H_\beta/H_\alpha)^{id}$ as a function of N_e, $N(HI)$, and $\tau(H_\alpha)$ for two different values of the electron temperature and two different values of the path length.

ACKNOWLEDGMENTS

We are grateful for the comments and suggestions of the referees, which have permitted improvement of our paper.

1. J. A. Pomarico, D. I. Iriarte, and H. O. Di Rocco, Eur. Phys. J., D **19,** 65 (2002).
2. D. I. Iriarte, J. Pomarico, and H. O. Di Rocco, Spectrochim. Acta, Part B **58,** 1945 (2003).
3. D. R. Bates, A. E. Kingston, and R. W. P. McWhirter, Proc. R. Soc. London, Ser. A **267,** 297 (1962).
4. D. R. Bates, A. E. Kingston, and R. W. P. McWhirter, Proc. R. Soc. London, Ser. A **270,** 155 (1962).
5. A. M. El Sherbini, H. Hegazy, and Th. M. El Sherbini, Spectrochim. Acta, Part B **61,** 532 (2006).
6. M. A. Gigosos, M. A. González, and V. Cardeñoso, Spectrochim. Acta, Part B **58,** 1489 (2003).
7. G. Bertuccelli, H. O. Di Rocco, and H. F. Ranea-Sandoval, J. Quant. Spectrosc. Radiat. Transfer **65,** 645 (2000).
8. G. Colonna, L. D. Pietanza, and M. Capitelli, Spectrochim. Acta, Part B **56,** 587 (2001).
9. D. Salzmann, *Atomic Physics in Hot Plasmas* (Oxford University Press, New York, Oxford, 1998).
10. A. Corney, *Atomic and Laser Spectroscopy* (Oxford University Press, Oxford, 1977).
11. R. D. Cowan, *The Theory of Atomic Structure and Spectra* (University of California Press, Berkeley, 1981).
12. I. I. Sobelman, L. A. Vainshtein, and E. A. Yukov, *Excitation of Atoms and Broadening of Spectral Lines* (Springer, Berlin, 1981).
13. L. Vriens and A. H. M. Smeets, Phys. Rev. A **22,** 940 (1980).
14. D. Mihalas, *Stellar Atmospheres* (W. H. Freeman, San Francisco, 1978), 2nd ed.
15. H. R. Griem, *Principles of Plasma Spectroscopy* (Cambridge University Press, New York, 1997).
16. W. Lotz, Z. Phys. **216,** 241 (1968).